

Journal of Materials Chemistry C

Accepted Manuscript



This is an *Accepted Manuscript*, which has been through the Royal Society of Chemistry peer review process and has been accepted for publication.

Accepted Manuscripts are published online shortly after acceptance, before technical editing, formatting and proof reading. Using this free service, authors can make their results available to the community, in citable form, before we publish the edited article. We will replace this *Accepted Manuscript* with the edited and formatted *Advance Article* as soon as it is available.

You can find more information about *Accepted Manuscripts* in the [Information for Authors](#).

Please note that technical editing may introduce minor changes to the text and/or graphics, which may alter content. The journal's standard [Terms & Conditions](#) and the [Ethical guidelines](#) still apply. In no event shall the Royal Society of Chemistry be held responsible for any errors or omissions in this *Accepted Manuscript* or any consequences arising from the use of any information it contains.



A light/pH/multiple ions-driven smart switchable module for computing sequential logic operations *via* resettable dual-optical readout†

Received 00th January 20xx,
Accepted 00th January 20xx

DOI: 10.1039/x0xx00000x

www.rsc.org/

Alok Kumar Singh‡^a, Promod Kumar Yadav‡^b, Niraj Kumari^b, Rajamani Nagarajan^a and Lallan Mishra*^b

A switchable module comprising of pendant pyridine groups, amide linkage and photoswitchable functionality (azobenzene) has been designed and characterized *via* full battery of physico-chemical techniques. The module has been exploited for ternary/binary data storage with non-destructive optical identity owing to its high photo-stability, brilliant reversibility, and chemical-/photo-switchability. Moreover the module exhibits sequential logic gate-based detection of multiple ions (Cu²⁺, CN⁻, F⁻ and I⁻) at ppm levels *via* “turn on” signature which potentially meets real-world-challenges through a simple synthetic route, rapid response, water based-activity, by-eye visualization, regenerative-action, high selectivity and the multiplereadout for precise analysis.

1. Introduction

Multi-stimuli responsive “smart molecules” illustrate huge promises in the field of molecular computing which has developed as a gifted alternative for information processing.¹ Compared with conventional silicon-based circuitries, molecular logics could result in smaller and additional proficient devices. Besides their potential functions in information processing and computing at the molecular level, their novel applications in the design of astute supramolecular materials, in drug delivery, and in clinical diagnostics have also been established.² In contrast to the combinatorial logic systems, where the input history is of no importance for the device function, sequential logic networks depend on both the input combination and the input sequence. Hence, these systems have memory potential.³ Therefore, mimicking sequential logic operations with multiple inputs using light, pH or multiple-ions and multiple outputs is more demanding and its growth is still in the infancy.^{1h,4} Furthermore, molecular keypad locks have received important awareness and there has been an impetus to improve these with a larger number of inputs as this can improve their safety level.⁵ The set–reset function in molecular digital systems is a significant action to assemble memory elements of sequential logic functions that have the opportunity to store information in a write–read–erasable

form.⁶ Photoswitchable molecules are key to accomplishing akin challenging tasks.⁷ Although a large number of photoswitchable systems are accessible, chemists have frequently made use of the azobenzene due to its convenient synthesis, fully reversible photo isomerization from *trans* to the *cis* form and binding of host has also been examined using receptor linked azobenzene systems.⁸ For these reasons, it has been extensively used to construct photoswitchable devices.

To date, the field of simultaneous detection of metal ions and anions has received significant care due to their important functions in many biological systems and the environment.⁹ Cu²⁺ is the third most abundant transition-metal ion in the human body (after Fe²⁺ and Zn²⁺) and their excess as well as deficiency can cause serious complications in body.¹⁰ On the other hand, CN⁻ ions despite of being very toxic have industrial uses.¹¹ F⁻ ions are added to drinking water/toothpastes for its valuable properties however higher dose of F⁻ are hazardous and can lead to dental or skeletal fluorosis.¹² I⁻ ions are one of the most biologically essential anions since it has prominent value in supporting neurological activity and thyroid gland function but higher dose of I⁻ are dangerous.¹³ So far, a number of well-designed synthetic probes specific for Cu²⁺ ion¹⁴, CN⁻ ion¹⁵, F⁻ ion^{15c,16} or I⁻ ion¹³ have been developed. Furthermore, a single probe capable of simultaneous detection of multiple ions (Cu²⁺, CN⁻, F⁻ and I⁻) has not been reported yet.

^a Department of Chemistry, University of Delhi, Delhi-110 007, India.

^b Department of Chemistry, Banaras Hindu University, Varanasi, India.

E-mail: lmishrabhu2@gmail.com

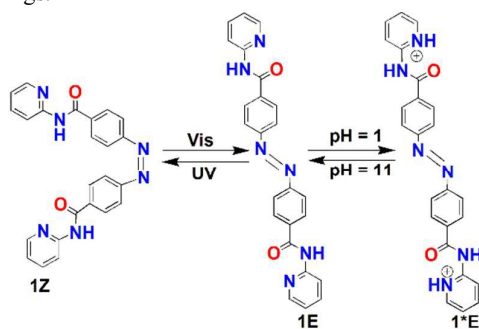
†Electronic Supplementary Information (ESI) available: Experimental details, ¹H NMR data and optical (absorption and emission) data for **1**. See DOI: 10.1039/x0xx00000x

‡These authors contributed equally to this work.

Taking these factors into account, we designed a novel light, pH and multiple ions-responsive molecule, **1** comprising proton and ions sensitive pendant pyridine groups, amide linkage and photoswitchable functionality (azobenzene) (Scheme 1). To the best of our knowledge, the molecule, **1** represent the first example of light/pH/multiple ions-driven smart switchable module for computing sequential logic operations via resettable dual-optical readout. Additionally our system (**1**) exhibits fast and selective sequential logic gate-based simultaneous detection of multiple-ions (Cu^{2+} , CN^- , F^- and I^-) at ppm levels *via* differential responses and “turn-on” signature using a single optical technique. This is also the first report for simultaneous detection of Cu^{2+} , CN^- , F^- and I^- in aqueous/non-aqueous media.

2. Results and discussion

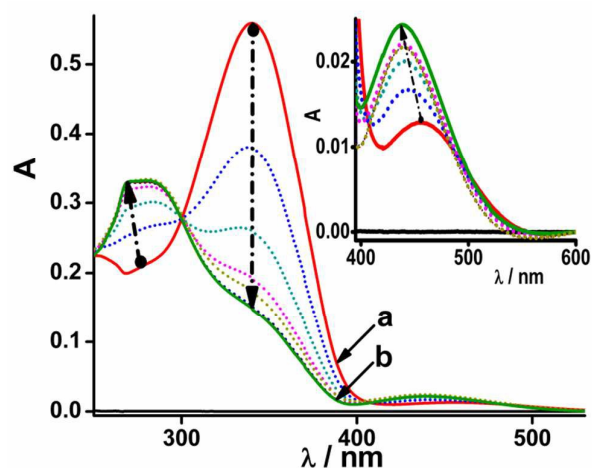
The photochrome **1** was prepared in good yield (68%) and characterized by full battery of physico-chemical techniques (Fig. S1-S4). The ^1H NMR spectrum of **1** exhibits peak at $\delta = 10.99$ ppm due to NH protons of amide group of **1** (Fig. S1).¹⁷ The proton nearby to pyridine nitrogen was shifted downfield extremely due to negative resonance of hetero-atom in the ring and observed at $\delta = 8.31$ ppm. Infrared spectrum shows peaks at $\nu = 1677$ and 1432 cm^{-1} due to C=O and N=N stretchings.¹⁸



Scheme 1 Representation of light- and pH-driven modulation of optical properties of **1**.

The UV-vis spectrum of **1** in dimethylformamide (DMF) displays a strong peak at $\lambda_{\text{max}} = 340\text{ nm}$ ($\epsilon = 55929\text{ M}^{-1}\text{ cm}^{-1}$) associated with a small intense peak in the visible region, $\lambda_{\text{max}} = 457\text{ nm}$ ($\epsilon = 1285\text{ M}^{-1}\text{ cm}^{-1}$), that can be assigned to $\pi\text{-}\pi^*$ and $n\text{-}\pi^*$ transitions respectively (Fig. S4).¹⁹ The photo-responsive molecule, **1** can be switched between compact (*Z*) and elongated (*E*) forms (Scheme 1) by UV and visible light. Irradiation of **1** (10^{-5} M , DMF) with UV light ($\lambda = 365\text{ nm}$) at different time intervals (1-14 min), led to the formation of its *cis* congener with hypochromic shift (3.8 fold) at $\lambda_{\text{max}} = 340\text{ nm}$ along with a hyperchromic shift (1.7 fold) at $\lambda_{\text{max}} = 270\text{ nm}$ (Fig. 1). Moreover, the peak at $\lambda_{\text{max}} = 457\text{ nm}$ was blue shifted ($\Delta\lambda = 19\text{ nm}$) along with an amplified intensity (1.9 fold). The original peak appeared again by irradiation of the UV treated solution with visible light (at $\lambda > 400\text{ nm}$) for 3 min. The isosbestic points at $\lambda = 300$ and 406 nm (Fig. 1) demonstrate that only two species are exchanging during the isomerization

process.²⁰ The ^1H NMR spectrum of **1** in DMSO-d_6 after treatment with UV light shows a slight upfield shift ($\delta = 8.09/8.22\text{ ppm}$ to $\delta = 8.02/8.18\text{ ppm}$) (Fig. S5) of *ortho* and *meta* hydrogens in azobenzene that demonstrates inclusive transformation of thermodynamically stable *trans* form to *cis*



form. Remarkably, **1** reaches to photostationary state in 14 min irradiation time, and protracted irradiation (up to 1 h) was unable to produce any further change in the spectrum as umpired by UV-vis spectroscopy. Nevertheless, significant signal-gain in the first 5 min (75%) was sufficient for observing the photochromism. The conformational changes were found to be of pseudo first order (Fig. S6).

Fig. 1 Absorbance changes of **1** (10^{-5} M , DMF) on revealing to UV light for 14 min (green line, b) and to visible light for 3 min (red line, a). The dotted lines provide as guide to the stepwise transformation following every 2 min irradiation. Inset: Magnified observation of absorbance changes for **1** at $\lambda_{\text{max}} = 457\text{ nm}$. Dotted arrows serve as guide to the eyes.

High photostability is vital factor for the photochromes, which permit large number of switching cycles for multiple uses. The reversibility and reusability of photochrome **1** was demonstrated for 10 cycles by alternating exposure to UV (for 14 min) and visible (for 3 min) lights (Fig. S7). Apparently, a $\sim 98\%$ conversion was observed for both isomeric forms. No significant hysteresis was observed after each “on/off” cycle confirming the excellent recovery process. For both the isomeric state, the shape and peak position of the absorption maxima (λ_{max}) remain unaffected. The *E* and *Z* forms are stable under ambient light and dark condition respectively, for at least 24 h as judged by UV-vis spectroscopy. The photochrome stability after long exposure of UV and visible light ($> 1\text{ h}$) and high on/off ratios ($\lambda_{\text{max}} = 270, 1.65$; $\lambda_{\text{max}} = 340, 3.75$; $\lambda_{\text{max}} = 457, 1.88$) offer integration of prototype non-volatile optical storage material in large optical window ($\lambda = 260\text{--}460\text{ nm}$).²¹ The $\pi\text{-}\pi^*$ band of **1** was found to be affected by temperature. At higher temperatures, the $\pi\text{-}\pi^*$ band of **1** was slightly blue-shifted with hyperchromic effect (Fig. S8). It is unlikely that this is due to interconversion between two

different trans conformations (e.g. a twisted and planar species) since isosbestic points are not observed.¹⁹

Stimulated by excellent photo-stability and photo-switchability of **1**, two-input sequential^{3,4,15b,15c} and combinatorial logic circuit²² have been constructed. The set-reset of **1** by UV and visible light can process information in the form of two-input sequential logic circuit. The variations in the absorbance at $\lambda_{\max} = 340$ nm (OUT1) and 270 nm (OUT2) have been captured as the outputs and the threshold values have been fixed to be 0.49 and 0.25, respectively. The absorbance greater than the threshold values are allocated as “1” and absorbance lesser than the threshold values are allocated as “0” corresponding to the “on” and “off” states of the readout signals, respectively. The logic circuit is planned in such a way that UV light works as I_1 whereas visible light works as I_2 (Sequence 1). When I_1 is high ($I_1 = 1$) the absorbance falls below the threshold level to give OUT1 = 0 and the stored information is “erased” from the system. While, successive addition of I_2 ($I_2 = 1$) again “writes” the information in the system as it recovers its initial absorbance with OUT1 = 1 (Fig. 2a). The reversible and reconfigurable sequences of set-reset logic operations in a feedback loop demonstrate the memory feature through OUT1 and OUT2. When the sequence command of the inputs is inverted and visible ($I_1 = 1$) is added before UV ($I_2 = 1$) (Sequence 2); a combinatorial²² logic circuit mimicking the functions of AND, NOT, OR and YES gates, is obtained (Fig. 2b).

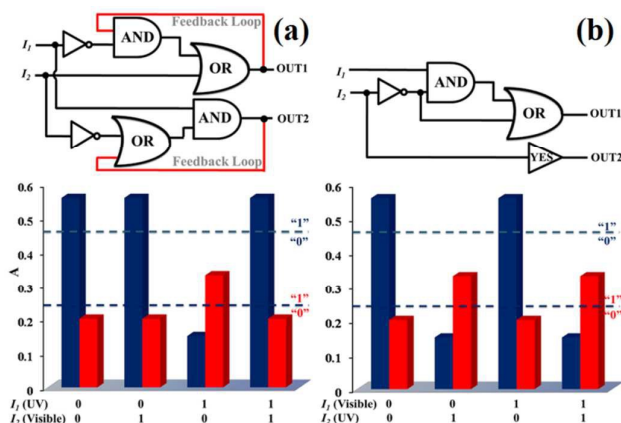


Fig. 2 Absorbance outputs of **1** in the presence of inputs viz. (a) I_1 (UV light) and I_2 (Visible light) and the corresponding two-input sequential logic circuit. (b) I_1 (Visible light) and I_2 (UV light) and the corresponding two-input combinatorial logic circuit. The dark blue and red bars depict OUT1 ($\lambda_{\max} = 340$ nm) and OUT2 ($\lambda_{\max} = 270$ nm) respectively. Dotted lines represent the threshold level of absorbance outputs.

The sequential logic operations could then be adopted to assemble a molecular keypad lock for securing information at molecular level. The UV and visible light are coded as “0” and “#”, respectively. Out of the potential permutations only the password “0#” could turn-on absorbance at $\lambda_{\max} = 340$ nm and unlock the device (Fig. S9).

The pH dependence of the UV-vis absorbance spectrum of **1** in DMF shows appearance of a new peak at $\lambda_{\max} = 275$ nm upon decreasing the pH from 11 to 1 (Fig. S10). The protonation of the pyridyl nitrogen at lower pH is said to be the most probable reason for the changes in the absorbance spectrum.¹⁹ However the spectra were remarkably unaltered by pH above pH 6.0 (Fig. S11). Therefore, protonation of the photoswitch should not be a hitch for biomolecular targets functioning near pH 7.

Fascinatingly, the emission intensity of **1** was tuned to display three distinct emission states upon varying the inputs (pH, UV and visible light) and thereby supporting the viability of **1** as an information storage module. For instance, the emission intensity of **1** (10^{-5} M, DMF) increases at $\lambda_{\max} = \sim 420$ nm (“turn on”, 57.7 fold) gradually by lowering the pH of the solution and reaches to optimum value at pH = 1 (Fig. 3, Fig. S11). This spectral perturbation can be assigned to the exclusive protonation of pyridyl nitrogen in **1**.¹⁹ In turn, the improved intensity evaporates regularly upon rising the pH of the solution and disappear at pH = 11. Moreover, upon imposing the UV light (for 14 min) to the solution of **1** at pH = 1, the emission intensity again “turn-on” additional 1.5 fold (Fig. 3). Furthermore, the original spectrum comes back upon exposure of visible light (for 3 min). The pH, UV and visible light-induced write/erase process has been executed for three consecutive cycles without any degradation in the intensity as umpired by fluorescence spectroscopy (Fig. 3, inset). Noticeably, **1** can produce three-state intensity changes i.e., **I** (intensity threshold = 45.12, **I**), **II** (intensity threshold = 205.28, **I** at pH = 1) and **III** (intensity threshold = 305.52, UV light treatment of **I** at pH = 1) under the stimuli pH and UV light respectively (Fig. 3). Furthermore overall optical alterations could be produced in a single step.

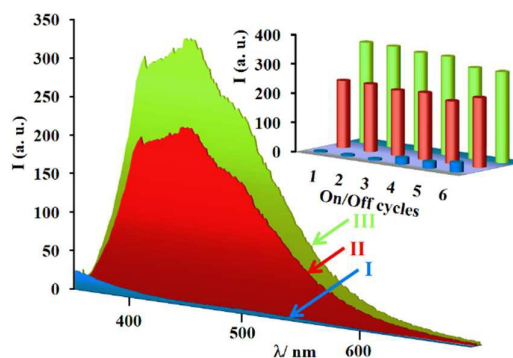


Fig. 3 Emission intensity of **1** (10^{-5} M, DMF, blue plot, **I**), at pH = 1 (red plot, **II**) and upon exposing with UV radiation for 14 min (light green plot, **III**). Inset: on/off cycles at $\lambda_{\max} = \sim 420$ nm as a function of pH (blue and red bars) and light (red and light green bars) ($\lambda_{\text{ex}} = 345$ nm).

Interestingly, the existence of three different states **I**, **II** and **III** could be exploited for incorporation of exchangeable binary and ternary memory states. To mimic the memory basics, intensity enhancement and reduction under each state can be considered as writing “1” and erasing “0” of data by

assuming the principle of binary logic.²³ Thus, binary memory states could be constructed by stimuli, HCl/NaOH/UV/visible light, capable of writing/ erasing the data for processing of multibits (“00”-“11”) of the same information. However, consecutive knocking viz. “00”, “10” and “11” might assemble a commutable ternary memory state under variable stimuli.

The cations and anions selective switching ability of **1** by applying inputs viz. cations (Ca^{2+} , Hg^{2+} , Co^{2+} , Zn^{2+} , Pb^{2+} , Mn^{2+} , Cd^{2+} , K^+ , Fe^{2+} , Ni^{2+} , Cr^{3+} , Cr^{6+} , Li^+ , Fe^{3+} , Na^+ , Mg^{2+}) and anions (Cl^- , F^- , NO_2^- , Br^- , PF_6^- , SO_4^{2-} , I^- , NO_3^- , CN^-) in aqueous/non-aqueous media could not produce any remarkable response in the absorbance, fluorescence and colour of **1** (*vide infra*). However, the UV-vis spectrum of **1**, shows immediate perturbation only in the presence of Cu^{2+} at ppm level concentrations associated with visible colour changes in real time (~5 s) from light yellow to dark yellow (Fig. 4a). Upon the addition of Cu^{2+} (20 ppm, H_2O) in **1** (10^{-5} M, DMF), π - π^* band at $\lambda_{\text{max}} = 340$ nm shows bathochromic ($\Delta\lambda = 21$ nm) and hypochromic shift (1.2 fold). Appearance of two isosbestic points at $\lambda = 316$ and 352 nm indicates formation of new species as an effect of addition of Cu^{2+} (Fig. 4a). Moreover, the addition followed a sigmoidal pattern (Fig. 4b, Fig. 4c). The output signals were stationary at 20 ppm for Cu^{2+} and show no deviation on increasing the concentration/reaction time up to three times. Excitingly, high on/off ratios (1.2 at $\lambda_{\text{max}} = 340$ nm and 1.3 at $\lambda_{\text{max}} = 361$ nm) combined with fast reaction rate permits an accurate quantification of Cu^{2+} in large optical window ($\lambda = 316$ - 470 nm) instead of monitoring at a single wavelength (Fig. 4). These results allow selective monitoring of Cu^{2+} via differential responses at different wavelengths.

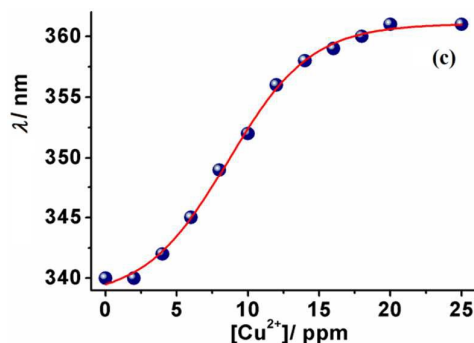
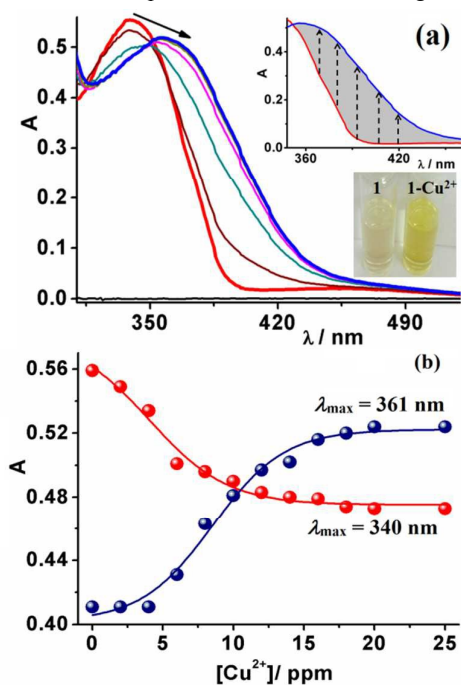
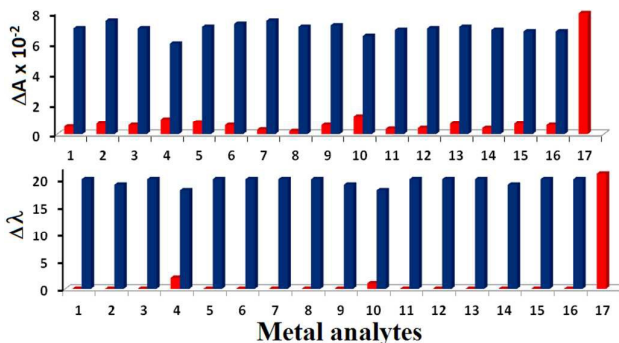


Fig. 4(a) Absorbance changes of **1** (10^{-5} M, DMF) (red) upon addition of input 2-25 ppm of Cu^{2+} (blue) in H_2O . Insets: entire area under the peak or any wavelength (dotted arrow) in the region 352-470 nm can be utilized for “turn-on” response. Photographs showing visual colour change in the solution of **1** (10^{-5} M, DMF) on addition of Cu^{2+} in H_2O . The observed dependence of (b) absorbance ($\lambda_{\text{max}} = 340$ nm, red balls, $R^2 = 0.97$ and $\lambda_{\text{max}} = 361$ nm, blue balls, $R^2 = 0.98$) and (c) wavelength ($R^2 = 0.99$) upon changing the ppm concentration of Cu^{2+} in H_2O is represented by sigmoidal shape. Note: “turn-on” readout allows measurement of low-concentration of the analyte and decreases the probability of false positive signal.

A brilliant probe needs to validate very selective identification in the competitive environment of analytes. The proposed probe **1** recognizes Cu^{2+} brilliantly in aqueous/non-aqueous media, since no significant variation was observed in absorption spectra (Fig. 5, red bars), and in colour (Fig. S12) upon addition of 20 ppm of inputs Ca^{2+} , Hg^{2+} , Co^{2+} , Zn^{2+} , Pb^{2+} , Mn^{2+} , Cd^{2+} , K^+ , Fe^{2+} , Ni^{2+} , Cr^{3+} , Cr^{6+} , Li^+ , Fe^{3+} , Na^+ and Mg^{2+} . Furthermore interference free detection of Cu^{2+} was achieved in



the presence of other test metal ions (Fig. 5, blue bars). Moreover, akin outcomes (~4-5%, experimental error) were achieved in non-aqueous medium.

Fig. 5 Representative bar chart showing absorbance and wavelength change at $\lambda_{\text{max}} = 340$ nm of **1** (10^{-5} M, DMF), upon addition of 20 ppm of various metal ions in H_2O (red bars). The blue bars depict interference test of 20 ppm of Cu^{2+} in the presence of 20 ppm of all other cations. 1 = Ca^{2+} , 2 = Hg^{2+} , 3 = Co^{2+} , 4 = Zn^{2+} , 5 = Pb^{2+} , 6 = Mn^{2+} , 7 = Cd^{2+} , 8 = K^+ , 9 = Fe^{2+} , 10 = Ni^{2+} , 11 = Cr^{3+} , 12 = Cr^{6+} , 13 = Li^+ , 14 = Fe^{3+} , 15 = Na^+ , 16 = Mg^{2+} and 17 = Cu^{2+} .

Recyclability of a probe must also be dealt with, as it resolves the scope of its service in cost-effective real-sample measurements. The “turned-off” and bathochromic shifted band of **1** by Cu^{2+} due to the formation of $\mathbf{1-Cu}^{2+}$ ensemble was immediately “turned-on” by addition of CN^- , F^- and I^- ions in the ppm concentration as low as 1 ppm in H_2O . The further addition of 20 ppm of $\text{CN}^-/\text{F}^-/\text{I}^-$ in the solution of $\mathbf{1-Cu}^{2+}$, not only enhanced the absorbance by nearly 100% but also brought back the initial light yellow colour of the solution instantly (Fig. 6). This possibly implies sequestering of Cu^{2+} by CN^- , F^- and I^- to potentially form $[\text{CuY}_x]^{n-}$ ($\text{Y} = \text{CN}^-/\text{F}^-/\text{I}^-$),²⁴ thus regenerating the probe **1** in the solution. None of the other examined anions could create any remarkable response in the absorbance of $\mathbf{1-Cu}^{2+}$ solution (Fig. S13). The system showed good reversibility for at least three cycles (Fig. 6). Thus probe **1** can be reset chemically by CN^- , F^- and I^- , indicating reversibility along with an added advantage of their fast, selective and by-eye detection at ppm-levels in H_2O . It is important to mention here that probes which can sense both CN^- and F^- simultaneously are extremely rare as evident by our recently published work.^{15c} To the best of our knowledge, this is the first report for simultaneous detection of CN^- , F^- and I^- in aqueous/non-aqueous media.

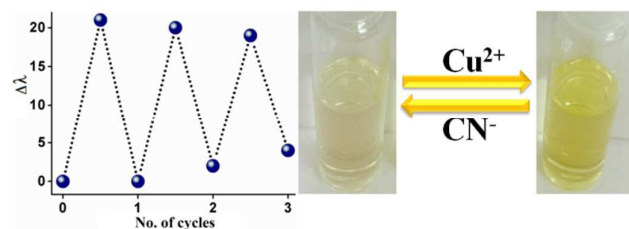


Fig. 6 The sensing-recovery cycles for **1** (10^{-5} M, DMF) upon addition of Cu^{2+} (20 ppm, H_2O) and subsequent regeneration by CN^- (20 ppm, H_2O). Dotted lines serve guide to eyes.

As explained, probe **1** act as an excellent “ON-OFF-ON” switch controlled by UV and visible light (*vide supra*). Similarly, motivated by its excellent selectivity (among large number of cations and anions), sensitivity, switchability, rapid and differential responses of **1** towards multiple-ions (Cu^{2+} , CN^- , F^- and I^-) in large optical window ($\lambda = 316\text{-}470\text{nm}$) (*vide supra*), two-input and three-output sequential and combinatorial logic circuits have been constructed. The multi-output generation by a single input could be potentially used for precise and defect-free recognition. In the set-reset of probe **1** by chemical inputs Cu^{2+} and CN^- the logic circuit is organized in such a way that Cu^{2+} works as I_1 whereas CN^- works as I_2 (Sequence 1). The deviations in the absorbance at $\lambda_{\text{max}} = 340$ nm (OUT1) and 361 nm (OUT2), and colour change by the naked eye (OUT3) have been captured as the outputs. The threshold values have been fixed to be 0.49 for OUT1 and 0.48 for OUT2. The absorbance more than the threshold values are assigned as “1” and absorbance lesser than the threshold values are assigned as “0” corresponding to the “on” and “off” states

of the readout signals, respectively. The colour change from light yellow to dark yellow is allocated as “0” and “1” respectively. When I_1 is high (considered as input signal “1-0”) the absorbance falls lower the threshold level at OUT1 while emerges at OUT2 and colour change to dark yellow at OUT3 (output signal “0-1-1”). However, successive addition of I_2 (input signal “1-1”) regains its initial absorbance and colour (light yellow) with signal pattern of “1-0-0” (Fig. 7a). The reversible and reconfigurable sequences of set-reset logic functions in a feedback loop demonstrate the memory feature through OUT1, OUT2 and OUT3. When the sequence order of the inputs is inverted and CN^- is added before Cu^{2+} (input signal “1-1”) (Sequence 2); a combinatorial logic circuit is obtained with signal pattern of “0-1-1” comprising of NOT, AND, OR and YES gates wired together (Fig. 7b). Moreover, the switchability of **1** controlled by Cu^{2+} and F^-/I^- can process information in the form of two input sequential and combinatorial logic circuit. Therefore, the sensing capabilities of probe **1** can be usefully continued to assemble molecular level logic circuits which can store the information planned by appropriate chemical inputs. All these investigations demonstrate that the probe can separately or simultaneously detect multiple-ions by using suitable outputs.

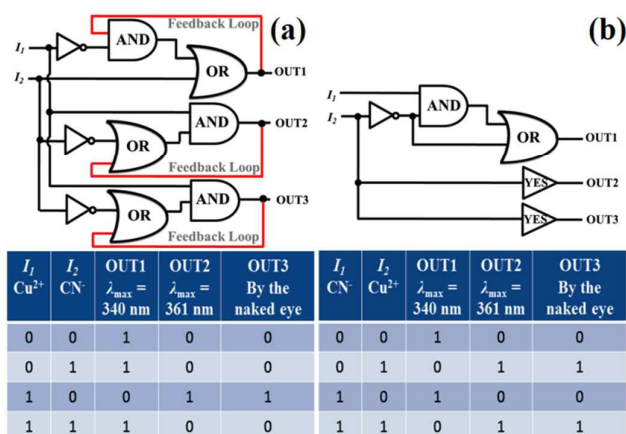


Fig. 7 (a) Truth table and sequential logic circuits displaying memory units with two inputs and three outputs in the presence of chemical inputs *viz.* I_1 (Cu^{2+}) and I_2 (CN^-). (b) Truth table and combinatorial logic circuits with two-inputs and three outputs in the presence of chemical inputs *viz.* I_1 (CN^-) and I_2 (Cu^{2+}).

Inspired by excellent switchability of **1** controlled *via* multiple-ions, molecular keypad locks with two inputs and one output has also been assembled. Out of the possible combinations password “*2”, “*7” and “*9” (* = Cu^{2+} , 2 = F^- , 7 = I^- and 9 = CN^-) could “turn-on” absorbance at $\lambda_{\text{max}} = 340$ nm and unlock the device. Any other key sequence, if pressed would fail to open the lock and produce an alarm (FALSE) signal (Fig. S14).

The probe was potential sufficient to detect Cu^{2+} in pool and tap water as demonstrated by proof-of-concept experiments. The wavelength changes at $\lambda_{\text{max}} = 340$ nm in sigmoidal shape as a function of ppm concentrations of Cu^{2+} till saturation limit (Fig. S15). The detection limit of **1** for Cu^{2+} came out to be 5.97

$\times 10^{-6} \text{ M}$,²⁵ thus providing an efficient system for monitoring traces of Cu^{2+} in environmental samples. Further, the binding constant computed for Cu^{2+} (Fig. S16) was obtained as $1.76 \times 10^9 \text{ M}^{-2}$, using Benesi-Hildebrand method.²⁶ Using Job's method of continuous variation of mole fraction, a stoichiometric ratio of 1:2 is observed for $\mathbf{1-Cu}^{2+}$ (Fig. S17). The nature of interactions has also been examined by ESI-MS (Fig. S18) which showed peak at 551.0087 for $[\mathbf{1}+2\text{Cu}^{2+}]$ along with a peak at 798.01 for $[\mathbf{1}+2\text{Cu}(\text{NO}_3)_2]$, which provided strong evidence for the formation of 1:2 complex between $\mathbf{1}$ and Cu^{2+} . In the IR spectrum of $\mathbf{1}$, a peak observed at 1677 cm^{-1} , assigned to its ' $>\text{C}=\text{O}$ ' group, changed to 1659 cm^{-1} on the addition of Cu^{2+} ions. The deshielding in peak position of ' $>\text{C}=\text{O}$ ' indicated its binding with Cu^{2+} ion. Moreover, the UV-vis data of $\mathbf{1-Cu}^{2+}$ showed a characteristic absorption band at 361 nm, indicating a trans configuration around the $\text{N}=\text{N}$ bond (*vide supra*). Based on these observations, the structure of a 1:2 complex between $\mathbf{1}$ and Cu^{2+} could be determined. In this complex, two Cu^{2+} may coordinate with nitrogen atoms of two pyridine groups and the oxygen atoms of the $\text{C}=\text{O}$ groups. The proposed interaction mode between $\mathbf{1}$ and Cu^{2+} is shown in Fig. S19.

3. Experimental section

3.1 Materials and Methods:

The majority of reagents used in this study was of highest purity (Sigma Aldrich) and were used without additional purification. Thin-layer chromatography (TLC) was executed using silica gel (60-120 mesh size). DMF was vacuum distilled over anhydrous MgSO_4 . Solvents such as CH_2Cl_2 , CHCl_3 were dried over P_2O_5 , Et_3N was dried over KOH, THF using sodium and benzophenone. ^1H NMR and ^{13}C NMR spectra were recorded on Jeol JNMEX 400p spectrometer at room temperature using DMSO-d_6 as solvent. All chemical shifts (δ) were recorded in ppm with reference to internal standard TMS. UV-vis spectra were recorded using an analytikjena SPECORD 250 by a quartz cuvette (path length = 1 cm, volume = 3 ml). Fluorescence spectroscopy experiments were executed on Varian Cary eclipse fluorescence instrument with a quartz cuvette (path length = 1 cm, volume = 3 ml). IR spectra were recorded at Perkin-Elmer FT-IR spectrometer in range $400\text{-}4000 \text{ cm}^{-1}$. The pH of the solution was fixed with EUTECH Instruments pH 510, calibrated with buffer solution of pH 4.00 and 9.00 before every measurement. The pH of test solution was adjusted with $\sim 10^{-3} \text{ M}$ HCl and NaOH solution in H_2O .

3.2 Synthesis of (E)-4,4'-(diazene-1,2-diyl)bis(N(pyridine-2-yl)benzamide) (1) (Scheme 1)

azobenzene 4,4'-dicarbonyl chloride (0.153 g, 0.5 mmol) dissolved in 10 ml dry THF. Triethylamine (0.150 g, 1.5 mmol) was added to 2-aminopyridine (0.235 g, 2.5 mmol) in 10.0 ml dry THF and solution of azobenzene 4,4'-dicarbonyl chloride was added dropwise. The reaction mixture was then stirred at room temperature

for 12 h. The orange precipitate obtained was filtered and dried. It was recrystallized by mixture of DMF/methanol. Yield: 67%; Melting Point: $>230 \text{ }^\circ\text{C}$. ^1H NMR (300 MHz, DMSO-d_6) δ (ppm): 7.96-8.12 (m, 10H, pyridine + azobenzene), 8.14 (d, 4H, pyridine), 8.31 (d, 2H, pyridine), 10.99 (s, 2H, NH); ^{13}C NMR (100 MHz, DMSO-d_6) δ (ppm): 122.76, 123.62, 129.24, 130.67, 140.41, 143.83, 153.58, 165.08; IR (cm^{-1} , KBr): $\nu_{(\text{C}=\text{O})}$ 1677 and $\nu_{(\text{N}=\text{N})}$ 1432; ESI-MS: $[\text{M}+1]^+$ Calculated for $\text{C}_{24}\text{H}_{18}\text{N}_6\text{O}_2$: 422.43, found: 423.2; UV-vis (10^{-5} M , DMF): $\lambda_{\text{max}} = 340 \text{ nm}$ ($\epsilon = 55929 \text{ M}^{-1} \text{ cm}^{-1}$); Anal. Calcd. for $\text{C}_{24}\text{H}_{18}\text{N}_6\text{O}_2$: C, 68.24; H, 4.29; N, 19.89. Found: C, 68.14; H, 4.07; N, 19.37.

4. Conclusions

In conclusion, module $\mathbf{1}$ was utilized for ternary/binary data storage with non-destructive optical identity owing to its high photo-stability, brilliant reversibility, and chemical/photo-switchability. The commutable binary and/or ternary state has verified precise control of stimuli over optical threshold and can recommend possible option to real memory devices. Moreover, we have developed the first probe capable of fast, selective and simultaneous detection of Cu^{2+} , CN^- , F^- and I^- ions at ppm levels in aqueous/non-aqueous media by "turn on" readout. The "by-eye" detection *via* obvious colour change makes probe $\mathbf{1}$ with economic significance. This study presents novel support that the logic gate strategy is an efficient approach for multiple-ions sensing. Outstandingly, our processor presents label-free detection among matrix of analytes and permits keeping uniqueness of information with no scope of mixing. Additional work is focussed toward customizing, miniaturizing, and more simplifying the detection device in order that such examination might become a valuable tool for Cu^{2+} , CN^- , F^- and I^- analysis in concerned households. Immobilization of this multitasking photochrome on a suitable substrate may improve its molecular convenience towards analytes and unlock stimulating potential in the pitch of new generation molecular-memory modules.²⁷

Acknowledgements

Financial assistance from DST (SERB/F/1424/2013-14), New Delhi and University of Delhi is gratefully acknowledged.

References

- (a) A. R. Pease, J. F. Stoddart, *Struct. Bonding* (Berlin) 2001, **99**, 189; (b) A. P. de Silva and S. Uchiyama, *Nat. Nanotechnol.*, 2007, **2**, 399; (c) M. Amelia, L. Zou and A. Credi, *Coord. Chem. Rev.*, 2010, **254**, 2267; (d) H. Tian, *Angew. Chem. Int. Ed.*, 2010, **49**, 4710; (e) G. de Ruiter and M. E. van der Boom, *Acc. Chem. Res.*, 2011, **44**, 563; (f) Y. Wu, Y. Xie, Q. Zhang, H. Tian, W. Zhu and A. D. Q. Li, *Angew. Chem. Int. Ed.*, 2014, **53**, 2090; (g) J. Andre'asson and U. Pischel, *Chem. Soc. Rev.*, 2015, **44**, 1053.

- (h) M. Chhatwal, A. Kumar, V. Singh, R. D. Gupta and S. K. Awasthi, *Coord. Chem. Rev.*, 2015, **292**, 30; (i) K. Chen, Q. Shu and M. Schmittel, *Chem. Soc. Rev.*, 2015, **44**, 136; (j) A.-M. Stadler and J.-M. P. Lehn, *J. Am. Chem. Soc.*, 2014, **136**, 3400; (k) B. Daly, J. Ling and A. P. de Silva, *Chem. Soc. Rev.*, 2015, **44**, 4203; (l) J. Ling, G. Naren, J. Kelly, D. B. Fox and A. P. de Silva, *Chem. Sci.*, 2015, **6**, 4472; (m) J. Ling, B. Daly, V. A. D. Silversson and A. P. de Silva, *Chem. Commun.*, 2015, **51**, 8403.
- 2 (a) A. P. de Silva, M. R. James, B. O. F. McKinney, D. A. Pears and S. M. Weir, *Nat. Mater.*, 2006, **5**, 787; (b) M. Elstner, K. Weisshart, K. Mullen and A. Schiller, *J. Am. Chem. Soc.*, 2012, **134**, 8098; (c) S. Pu, D. Jiang, W. Liu, G. Liu and S. Cui, *J. Mater. Chem.*, 2012, **22**, 3517; (d) S. Pu, Z. Tong, G. Liu and R. Wang, *J. Mater. Chem. C*, 2013, **1**, 4726 (e) D. S. Kim, V. M. Lynch, J. S. Park and J. L. Sessler, *J. Am. Chem. Soc.*, 2013, **135**, 14889; (f) F. Pu, E. Ju, J. Ren and X. Qu, *Adv. Mater.*, 2014, **26**, 1111; (g) K. Zhu, J. Shen, R. Dietrich, A. Didier, X. Jiang and E. Martlbauer, *Chem. Commun.*, 2014, **50**, 676; (h) D. Kim and T. S. Lee, *Chem. Commun.*, 2014, **50**, 5833; (i) K. S. Hettie, J. L. Klockow and T. E. Glass, *J. Am. Chem. Soc.*, 2014, **136**, 4877; (j) Y. Liu, Y. Zeng, L. Liu, C. Zhuang, X. Fu, W. Huang and Z. Cai, *Nat. Commun.* 5:5393doi: 10.1038/ncomms6393 (2014); (k) L. Feng, Z. Lyu, A. Offenhusser and D. Mayer, *Angew. Chem. Int. Ed.*, 2015, **54**, 7693.
- 3 (a) G. de Ruiter, E. Tartakovsky, N. Oded and M. E. van der Boom, *Angew. Chem. Int. Ed.*, 2010, **49**, 169; (b) S. Pramanik, V. Bhalla and M. Kumar, *ACS Appl. Mater. Interfaces*, 2014, **6**, 5930.
- 4 (a) M. Irie, T. Fukaminato, K. Matsuda and S. Kobatake, *Chem. Rev.*, dx.doi.org/10.1021/cr500249p; (b) X. -J. Jiang and D. K. P. Ng, *Angew. Chem. Int. Ed.* 2014, **53**, 10481.
- 5 (a) D. Margulies, C. E. Felder, G. Melman and A. Shanzer, *J. Am. Chem. Soc.*, 2007, **129**, 347; (b) S. Chen, Z. Guo, S. Zhu, W. Shi and W. Zhu, *ACS Appl. Mater. Interfaces*, 2013, **5**, 5623; (c) C. P. Carvalho, Z. Domínguez, J. P. Da Silva and U. Pischel, *Chem. Commun.*, 2015, **51**, 2698.
- 6 (a) M. Kumar, N. Kumar and V. Bhalla, *Chem. Commun.*, 2013, **49**, 877; (b) X. Mei, G. Wen, J. Wang, H. Yao, Y. Zhao, Z. Lin and Q. Ling, *J. Mater. Chem. C*, 2015, **3**, 7267.
- 7 (a) J. Andreasson, U. Pischel, S. D. Straight, T. A. Moore, A. L. Moore and D. Gust, *J. Am. Chem. Soc.*, 2011, **133**, 11641; (b) J. Yoon, *Angew. Chem. Int. Ed.*, 2014, **53**, 6600; (c) J. Yoon and A. P. de Silva, *Angew. Chem. Int. Ed.*, 2015, **54**, 2–5.
- 8 (a) Q. M. Zhang, X. Li, M. R. Islam, M. Wei and M. J. Serpe, *J. Mater. Chem. C*, 2014, **2**, 6961; (b) J. Garcia-Amoros, M. Reig, A. Cuadrado, M. Ortega, S. Nonell and D. Velasco, *Chem. Commun.*, 2014, **50**, 11462; (c) M. Dong, A. Babalhavaeji, M. J. Hansen, L. Kalman and G. A. Woolley, *Chem. Commun.*, 2015, **51**, 12981; (d) L. He, G. Wang, Q. Tang, X. Fu and C. Gong, *J. Mater. Chem. C*, 2014, **2**, 8162.
- 9 (a) S. K. Kim and J. L. Sessler, *Acc. Chem. Res.*, 2014, **47**, 2525; (b) M. Ciardi, A. Galan and P. Ballester, *J. Am. Chem. Soc.*, 2015, **137**, 2047.
- 10 H. M. Kim and B. R. Cho, *Chem. Rev.*, 2015, **115**, 5014.
- 11 B. A. Logue, D. M. Hinkens, S. I. Baskin and G. A. Rockwood, *Crit. Rev. Anal. Chem.*, 2010, **40**, 122.
- 12 K. L. Kirk, *Biochemistry of the Elemental Halogens and Inorganic Halides*, Plenum, New York, 1991.
- 13 A. Mitra, A. Pariyar, S. Bose, P. Bandyopadhyay and A. Sarkar, *Sens. Actuators B*, 2015, **210**, 712.
- 14 (a) R. Kumar, Y. O. Lee, V. Bhalla, M. Kumar and J. S. Kim, *Chem. Soc. Rev.*, 2014, **43**, 4824; (b) R. Wu, S. Zhang, J. Lyu, F. Lu, X. Yue and J. Lv, *Chem. Commun.*, 2015, **51**, 8078; (c) H. Jia, S. Pu, C. Fan, G. Liu and C. Zheng, *Dyes Pigm.*, 2015, **121**, 211; (d) S. Cui, S. Pu and Y. Daia, *Anal. Methods*, 2015, **7**, 3593; (e) S. Xia, G. Liu and S. Pu, *J. Mater. Chem. C*, 2015, **3**, 4023.
- 15 (a) F. Wang, L. Wang, X. Chen and J. Yoon, *Chem. Soc. Rev.*, 2014, **43**, 4312; (b) M. A. Kaloo, R. Mishra and J. Sankar, *J. Mater. Chem. C*, 2015, **3**, 1640; (c) A. K. Singh, *RSC Adv.*, 2015, **5**, 30187.
- 16 L. Gai, J. Mack, H. Lua, T. Nyokong, Z. Li, N. Kobayashi and Z. Shen, *Coord. Chem. Rev.*, 2015, **285**, 24.
- 17 R. M. Silverstein and F. X. Webster, *Spectrometric identification of organic compounds*, John Wiley & Sons, 1998.
- 18 K. Nakamoto, *Infrared and Raman Spectra of Inorganic and Coordination Compounds*, John Wiley & Sons, 2008.
- 19 A. A. Beharry, O. Sadoyski and G. A. Woolley, *J. Am. Chem. Soc.*, 2011, **133**, 19684.
- 20 Y. Yang, R. P. Hughes and I. Aprahamian, *J. Am. Chem. Soc.*, 2012, **134**, 15221.
- 21 A. S. Matharu, S. Jeeva and P. S. Ramanujam, *Chem. Soc. Rev.*, 2007, **36**, 1868.
- 22 A. Kumar, M. Chhatwal, A. K. Singh, V. Singh and M. Trivedi, *Chem. Commun.*, 2014, **50**, 8488.
- 23 T. Gupta and M. E. van der Boom, *Angew. Chem., Int. Ed.*, 2008, **47**, 5322.
- 24 X. Lou, D. Ou, Q. Li and Z. Li, *Chem. Commun.*, 2012, **48**, 8462.
- 25 A. Kumar, A. K. Singh and T. Gupta, *Analyst*, 2013, **138**, 3356.
- 26 H. A. Benesi and J. H. Hildebrand, *J. Am. Chem. Soc.*, 1949, **8**, 2703.
- 27 A. Kumar, M. Chhatwal, P. C. Mondal, V. Singh, A. K. Singh, D. A. Cristaldi, R. D. Gupta and A. Gulino, *Chem. Commun.*, 2014, **50**, 3783.

Graphical Abstract

